THERMAL STUDY

PILOT'S PRESSURE SUIT

THERMAL STUDY

OF THE

S901G

PILOT'S PROTECTIVE ASSEMBLY

JAR-856-733

**On file USAF release
instructions apply.**

COMMENTS BY

LOW SPEED

1. THE INITIAL ASSUMPTION THAT SOLAR RADIATION IS THE MAIN CAUSE OF DISCOMFORT IS WRONG. THE PROBLEM IS PRIMARILY DUE TO 300 TO 400° C COCKPIT WALL & GLASS TEMPERATURE. THIS RESULTS IN A HEAT RADIATION OF DIFFERENT WAVELENGTHS THAN THOSE USED IN THE TEST. IF SOLAR RADIATION WAS A PROBLEM, FLIGHT IN A SAGE GREEN FLYING SUIT UNDER A BUBBLE CANOPY AT 50,000' WOULD BE UNBEARABLE.

HEAT RADIATED FROM THE $^{300-400°}$ COCKPIT WALLS & GLASS IS UNCOMFORTABLE IN SPITE OF AMBIENT COCKPIT AIR BEING AT 50 - 60° F LEVELS.

2. SUGGEST THE NEXT TEST IS RUN WITH A YEAR OLD (OR MORE) SAMPLE OF ALUMINIZED FABRIC THAT HAS BEEN IN HARD SERVICE USE. COMPARE THIS WITH NEW ALUMINIZED FABRIC & ALSO A PURE WHITE FABRIC.

3. I BELIEVE A ^SMOOTH PURE WHITE ^FABRIC THAT CAN BE KEPT WHITE BY WASHING WILL BE CHEAPER & MORE EFFECTIVE IN THE LONG

RUN THAN ALUMINIZED FABRIC.

ENCL #

OXC-8620

COPY 1 OF 2

JAR-856-733

THERMAL STUDY

OF THE

S901G

PILOT'S PROTECTIVE ASSEMBLY

3 May 1965

Chem. Lab B

TABLE OF CONTENTS

LIST OF FIGURES

Chem. Lab B

LIST OF GRAPHS

LIST OF TABLES

LIST OF CHARTS

Chem. Lab B

1.0   INTRODUCTION:

This report is the result of effort undertaken to
date to determine the level of protection afforded
the pilots using the BASIC Pilot's Protective Assembly
(P.P.A.) on typical test and training missions.
Reports that heat leak through the P.P.A. from the
cockpit ambient has been approaching a critical
level prompted the assignment of this task.

The solar radiation available in the operating
altitudes and the percentage of that radiation enter-
ing the cockpit are suspected to have an enormous
effect on thermal balance of the pressure suit and
consequently on the comfort of the pilot.

Most solar heat is assumed to be entering through
the cockpit windows and impinges directly on the
aluminized surface of the P.P.A.

The solar radiation experienced consisted of earth's
reflectivity known as the albedo the solar flux
generated directly from the sun. This solar radia-
tion can produce as much as $250^\circ F$ temperature on
the surface of the thermal garment within ten minutes
of the mission. To obviate this phenomenon, the
P.P.A. consisted of a thermal garment and a constant
cooling ventilation system.

Until just recently the thermal garment used con-
sisted of 4.2 oz./sq. yd. HT-1 "NOMEX" which was
aluminized and served as the heat shield combined
with a composite as shown on page 13, Fig. 4.

Reflective values of this material were on the aver-
age of 70 to 80% between 200 and 2500 millimicrons
wavelength. The emissivity value was approximately
.2 provided that the film was dust free and not ex-
posed to oxidation.

The thermal garment fabricated from such material was highly heat resistant, physically strong and non-flammable. However, because the fabric was loosely woven, the reflective film was easily distorted causing flake-off, cracks and consequent deficiency in heat balance due to reflectivity loss.

Development of new HT-1 "NOMEX" fabric and aluminum coatings have been in process and performance of the new material is reflected in this report.

2.0 TEST PROGRAM:

2.1 Object:

This study was undertaken to determine quan-
titatively the radiant heat flux required to
develop a surface temperature of 200 to 250°F
on or near the surface of the suit. The in-
ternal heating effect of this heat flux was
also studied under various air-flow conditions.

Notation was made as to the variation in heat-
ing rates of various simulated skin positions.
These positions simulated the skin in a loose
fitting suit or area and where the skin com-
presses the suit layers such as a bent elbow
or knee.

2.2 Test Equipment:

2.2.1 Environmental System:

The test equipment was set up around
a Kinney Vacuum Pump, Model #KDTG-3P
as a core (see Fig. 5). Outside the
pump chamber the following equipment
was arranged:

1. air supply
2. air regulator
3. flow meter
4. monometer
5. needle valve
6. gas feed through
7. gas feed through for ozone
   titrator
8. ozone titrator

Inside the chamber the thigh section of
the suit was located under the IR and UV
lamps. A cross-section view of the test
specimen is shown in Fig. 4 along with
the location of the five (5) thermo-
couples used.

Three thermocouples were located on the exterior of the suit section, identified as "A","B", and "C", one each at the right, center and extreme left. Two thermocouples were located inside the suit section. One was attached to the cotton underwear material directly under the outside center thermocouple, the other was attached to a plate moveable on a vertical axis in the center of the test specimens.

This plate was essential in the performance of the test, for it was this plate that represented the skin surface of a man wearing the suit. The plate was made moveable so that the test could be made with a space between skin position and underwear material, representing the suit over a loose fitting portion of the body. The plate was then moved up to the insulating materials as required to assimulate actual conditions. This position represented the skin pressing against the insulation on an area such as a bent elbow or knee.

The two inside thermocouples' leads were fed out of the chamber through the exhaust feed through. The three outside thermocouples left the chamber by way of a special thermocouple feed through. Outside the chamber, the thermocouple wires were connected through a switch box to a "Varian" temperature recorder. (see Fig. 1)

2.2.2   Ozone Titrator:

The OREC manual ozone instrument was used to determine the percentage of ozone available within the high altitude chamber during the test.

The OREC ozone measurement instrument,
as shown in Figs. 6 and 7, was used
throughout the test program. The in-
strument employed for this measurement
of ozone was based on a chemical titra-
tion principle. The concept of measure-
ment was based on the quantitative re-
lease of Iodine (I_2) from buffered
aqueous solution of potassium iodide
(KI) according to the reaction:

$$O_3 + 2KI + H_2O \rightarrow O_2 + I_2 + 2KOH$$

A very low voltage was impressed across
a set of platinum electrodes which was
inserted in the aqueous solution.

In the presence of Iodine the current
will flow according to the electrodes
increasing the value as the concentration
of Iodine increases. This instrument
contains a microammeter to indicate the
current flow.

2.2.3   Spectrophotometer:

In order to analyze the reflectivity
value of aluminized reflective material,
the Beckman IR4 Spectrophotometer was
used for this purpose.

This instrument is modified with track-
ing accurace control (TAC) comparable
to the IR7 Spectrophotometer and is
equipped with the VAR and ATR reflecto-
meter attachment.

The instrument operates in single and
double beam with a monocromatic double
50 cm. focal length, slit 25 high with
bilateral from 0 to 3 mm. and a chart
linear intransmittance and wavelengths.
The monocrometer and reflectance lense
are all of sodium chloride (NaCl) and
equipped with interchangeable prisms

within an accurate wavelength from 2
to 15 microns. The wavelength re-
flectivity is equal to .005 microns
and has a resolving power of .01 to
10 microns. The wavelength skill
expansion in in./microns are within
.4, 0.3, 1, 1.6, 2.0, 2.5, 4.0, 5.0
and 10.

2.3 Procedure:

2.3.1 Environmental Test Procedure:

The chamber was first pumped down to
3,000 microns and all temperatures were
recorded. The air flow was regulated
and the temperature again recorded.
The lamps were then turned on and
temperature readings taken every two
(2) minutes for a 30 minute test dura-
tion. Power consumption of the lamps,
flow rate and chamber pressure were
also checked and recorded every two
(2) minutes.

During a typical test the concentration
of ozone in the chamber generated from
the UV lamp was measured. The measure-
ment was made with an OREC, Model MSA-2
Manual Ozone Titration Apparatus. This
ozone was generated from water and oxygen
present from offgassing and system leaks.
In the presence of the UV lamp, ozone
was generated according to the chemical
equation:

$$6H_2O + 3O_2 \xrightarrow{UV} 2H_2O + 4H_2 + 2O_2 + 2O_3$$
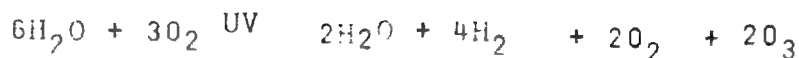
2.3.2 Determination of Reflectivity:

All materials described in this report
of reflective nature and used as exterior
coverall were evaluated initially and
after exposure to the environment to establish
the reflectivity value or the percentage
of degradation.

Chem. Lab B

First of all the instrument was bal-
anced with the reference aluminum
mirror with a setting of high resolu-
tion and tested to determine the effect
of angular impingment as shown on
Chart 1.

The second such test was conducted us-
ing the ATR attachment which consisted
of sodium chloride prism. (see
Chart 4)

It was established in the initial environ-
ment that the most frequent and effcient
solar impingment occurred at 45°, there-
fore, throughout the test this angle
was used.

Several single beam reflectance measure-
ments were made to establish resolutions
at the maximum energy available for mat-
erials which were not of the best re-
flective surface. (see Chart 7)

The samples were taken from the most
directly exposed areas which were located
directly under the solar lamp and thermo-
couple "A" as shown in Fig. 5.

No special attention was given in pre-
paration of samples for the reflectivity
study, such as surface cleaning or de-
contamination. This was purposely done
to obtain realistic data which would be
experienced in practical use.

2.4 Test Specimens and Test Numbers:

TEST NUMBERS	MATERIALS TESTED AND CONDITIONS
1a	Standard aluminized HT materials, 3M standard process scotch shield – low flow rate and uncompressed composite.
1b	Same as 1a only with high flow rate.
1c	Same material as 1a with low flow and compressed composite.
1d	Same material as 1a with high flow and compressed composite.
2a	DC Heat Shield Type 3, ACS-1440C with B film. First high temperature cure system, low flow rate and uncompressed composite.
2b	Same material as 2a with high flow rate and uncompressed composite.
2c	Same material as 2a with low flow rate and compressed composite.
2d	Same material as 2a with high flow rate and compressed composite.
3a	3M Scotch Shield, stiff material over dacron and wool insulation – low flow rate and uncompressed composite.
3b	Same material as 3a with high flow and uncompressed composite.
3c	Same material as 3a with low flow and compressed composite.
3d	Same material as 3a with high flow and compressed composite.

TEST NUMBERS	MATERIALS TESTED AND CONDITIONS
4a	Stern & Stern 6 oz. HT fabric over composite of 2a - low flow rate and uncompressed composite.
4b	Same material as 4a with high flow rate and uncompressed composite.
4c	Same material as 4a with low flow rate and compressed composite.
4d	Same material as 4a with high flow rate and compressed composite.
5a	Stern & Stern 6oz. HT fabric over dacron and wool insulation - low flow rate and uncompressed composite.
5b	Same material as 5a with high flow rate and uncompressed composite.
5c	Same material as 5a with low flow rate and compressed composite.
5d	Same material as 5a with high flow rate and compressed composite.

NOTE: The materials listed in the above tests are in addition to one layer of HT link net, one layer of bladder material, one layer of sage green oxford nylon and one layer of cotton underwear material. (see Fig. 4)

FIGURE #1

High altitude environmental and thermal evaluation
set up for suit thigh cross section.

Chem. Lab B

FIGURE #2

Suit thigh cross section in high altitude chamber.

Chem. Lab B

FIGURE #3

Blow out of suit thigh cross section after the
first phase of environmental testing.

FIGURE #4

CONSTRUCTION OF THIGH SECTION OF TYPICAL S-901 HIGH
ALTITUDE SUIT

Numbers

1
2
3
4   Thermocouples   Moveable
5   Plate

Air Flow   Exhaust
  Inlet

Open for Interior
     Air Flow
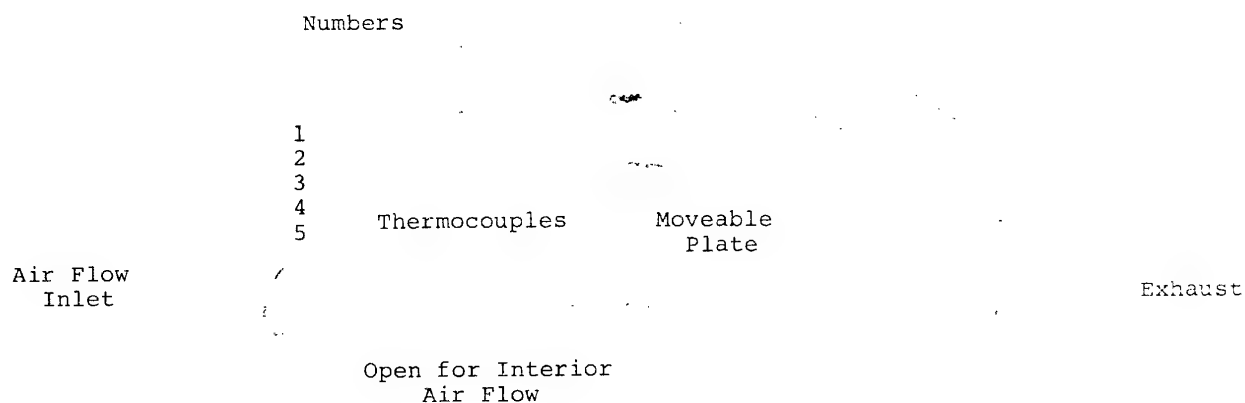
LAYERS:
1.)   Coverall Material
2.)   Restraint HT-1 Link Net
3.)   Bladder P-1807A
4.)   Liner, Nylon Blue
5.)   Underwear Material, Cotton

FIGURE #5   TEST EQUIPMENT

Vacuum Chamber

IR Lamp

UV Lamp

Flow Meter

Regulator   Monometer

Needle Valve   Thermocouple   To Vacuum
                        Gage   Pump

Air Supply

Temperature   ⟶
Recorder

Thermocouple
Switch Box
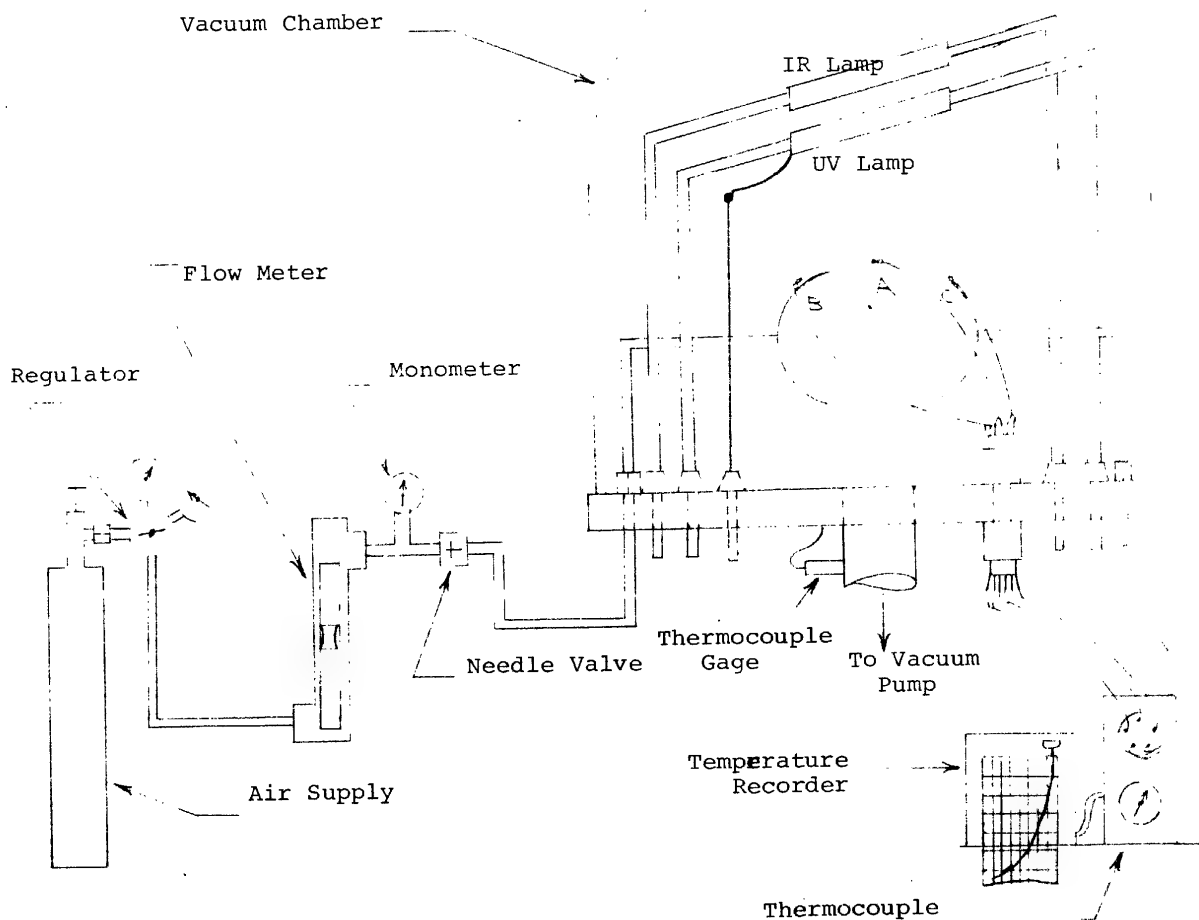
FRONT VIEW   FIGURE #6
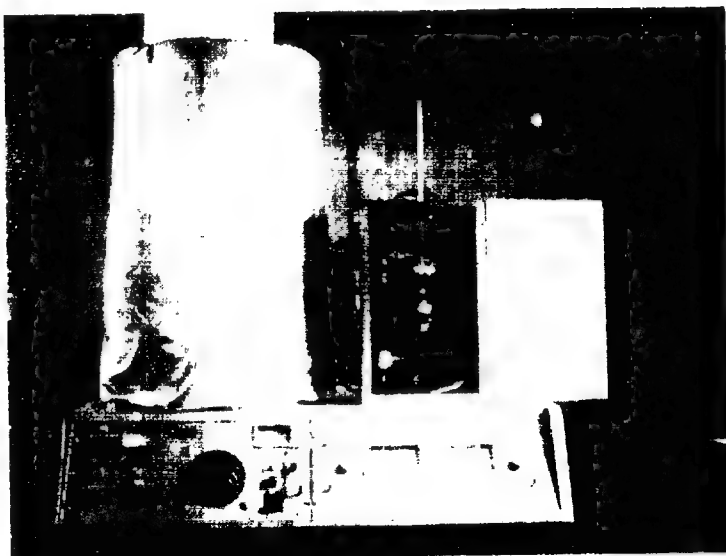
OZONE TITRATOR ATTACHED TO
ALTITUDE CHAMBER

FIGURE #7   SIDE VIEW

3.0 CALCULATIONS:

3.1 Theory and Equations for Calculations of
Radiant Energy from IR Lamp:

The energy radiated from the IR source is dir-
ectly proportional to the absolute temperature
of the filament. It can be found by the use
of the Stefan-Boltzmann Law:

1. $W = \epsilon\sigma T^4$

WHERE: W = radiated energy in watts/cm.^{2} source
ϵ = emissivity of the radiator
σ = Stefan-Boltzmann Constant =
5.673×10^{-12} watts/(cm^2) $(deg.^4)$
T = temperature in degrees Kelvin

The principle wavelength can be calculated from
Wien's Displacement Law which is derived from
the derivative of Planck's Law solved for a
maximum. Wein's Displacement Law is:

2. $\lambda_m T = K$

WHERE: λ_m = wavelength in microns where W_2
is a maximum
K = constant $2897\,^{\circ}K$ micron (see Graph 3)

Substitution of Wein's Displacement in Planck's
Law yeilds a simplified equation for finding
the power given at the principle wavelength
λ_m.

3. $W\lambda_m = 1.3T^5 \times 10^{-15}$

3.2   Example of Calculations:

If the applied voltage to the lamp was 77 volts, the color temperature would be approximately 2250°K, as shown on Graph 2, and the real temperature would be 2200°K. At this temperature, the total emissivity of Tungsten is 0.279. The radiating surface area of the lamp is 6.5 cm.^{2} Therefore, to find the total radiated energy apply the Stefan-Boltzmann Law:

$W = \varepsilon\sigma T^4$
$W = .279 \times 5.673 \times 10^{-12} \times 2200^4$
$W = 37.08$ watts/cm^2 or for
6.5 cm^2 of source area total
$W = 45.74 \dfrac{\text{watts}}{\text{cm}^2} \times 6.5$ cm$^2 = 241$ watts

From Tungsten's Spectral Distribution graph on page 24, Table V, it can be seen that 156.5 watts are emitted at the peak of radiation wavelength of 1.25 microns.

Of the approximately 241 watts of energy emitted, only a certain portion comprised the heat flux incident at the thermocouple location under study. This heat flux, "J", can be determined by the following equation:

4. $J = \dfrac{\theta}{360} \times \dfrac{1}{d^2} \times W_t$

WHERE: d = distance in cm. from temperature to specimen
θ = angle formed by incident rays from lamps which include total specimens which are under study. (see Fig. 8 on page 18)

FIGURE 8

<u>END VIEW OF LAMP AND
THERMOCOUPLE LOCATION</u>

8"

2"

← Specimen
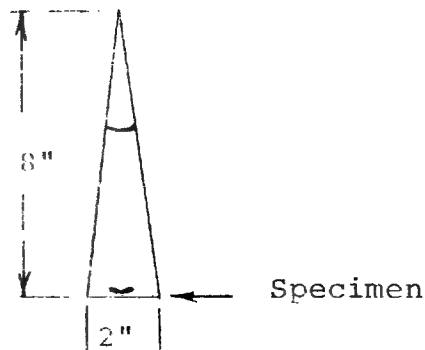
In the problem under discussion, the heat flux would be:

$$J_{IR} = \frac{14.4}{360} \times \frac{1}{[(2.54)(8)]^2} \times 241$$

$$J_{IR} = .0233 \text{ watts/cm}^2$$

<u>CALCULATION OF UV ENERGY</u>

From the spectral distribution table on page 26, it can be seen that a total of 44.15 watts are radiated from the UV lamp in the UV and visible wavelength region. This energy transmitts an incident heat flux according to equation #4. (see Graph 4)

$$J_{UV} = \frac{\theta}{360} \times \frac{1}{d^2} \times W_t$$

$$J_{UV} = \frac{14.4}{360} \times \frac{1}{(2.54 \times 8)^2} \times 44.15$$

$$J_{UV} = .0044 \text{ watts/cm}^2$$

The total heat flux is then the sum of J_{IR} and J_{UV}

Total J = .0233 + .0044 = .0277 watts/cm^2

Although this figure was derived from an original data reading of 77 volts, the final heat flux, "J", could be used for approximate value of 76-78 volts. This is due to the approximation and extrapulation made as discussed on page 41.

3.3   Flow Rate Determination:

Flow rates were determined by volume ratio. That is, the volume of the suit section used was approximately 0.395 ft.³ as compared to an approximate air volume of a suit with a man in it equal to 1.83 ft.³. The minimum and maximum flow rates for the suit was 8 to 18 scfm respectively. These flow rates were reduced to 1.732 & 3.88 scfm by direct ratio for the suit section tested. However, with the equipment used, the lowest flow rate that could be maintained was 2.7 scfm and this was the value used as the low flow rate.
(see Tables I and II)

(Test Flow Rate)   =   0.216 (Suit Flow Rate)

TABLE I
CONVERSION TABLE OF FLOWS IN SCFM

High flow 18 scfm suit flow   =   3.88 scfm test flow rate

Low flow 8 scfm suit flow   =   1.73 scfm test flow rate

Low flow used 12.5 scfm   =   2.7 scfm test flow rate

TABLE II
CONVERSION TABLE OF FLOWS IN LBS/MIN

Test Specimen:

FLOW RATE SCFM	PRESSURE IN Hg	STATIC VOL. @ 65°F	FLOW IN LBS/MIN
2.7	5.3	.033	.223
3.88	20.3	.047	.454

Equivalent in Actual Suit:

| 12.5 | 0.509 | .130 | .568 |
| 18.0 | 3.05 | .161 | 1.583 |

TABLE III

ALTITUDE AND RELATED PRESSURE

ALTITUDE IN FEET	PRESSURE IN MICRONS
0	760 X 10^3
2500	694 X "
5000	632 X "
10,000	522 X "
20,000	349 X "
30,000	226 X "
40,000	141 X "
50,000	87.49 X "
60,000	54.24 X "
70,000	33.65 X "
80,000	21.01 X "
90,000	13.21 X "
100,000	8.36 X "
110,000	5.33 X "
120,000	3.45 X "
130,000	2.27 X "
140,000	1.51 X "
150,000	1.02 X "
160,000	0.697 X "
170,000	0.478 X "

PRESSURE USED

GRAPH #1

ALTITUDE VS. PRESSURE

Altitude in
feet X 1000

100

90

80

70

60

50

40

PRESSURE IN MICRONS
X 10^4

30
25   24 23   22   21   20   19   18   17   16   15   14   13   12   11 10   9   8   7   6   5   4   3   2   1   0

TABLE IV

LAMP VOLTAGE VS. COLOR TEMPERATURE

VOLTAGE	COLOR TEMP. ^{O}F	COLOR TEMP. ^{O}K
15	1840	1277
20	2165	1458
25	2400	1588
30	2570	1683
35	2800	1811
40	2955	1897
45	3100	1977
50	3200	2033
55	3290*	2083
60	3380*	2133
65	3460*	2177
70	3525*	2213
75	3575*	2241
80	3610*	2261
85	3648*	2280
90	3668*	2293

* Indicates extrapulated values

Chem. Lab B

APPLIED LAMP VOLTAGE
VS.
IR COLOR TEMPERATURE

COLOR TEMPERATURE
DEGREES KELVIN

X—X   Test Data

⊗—⊗   Extrapulated Values
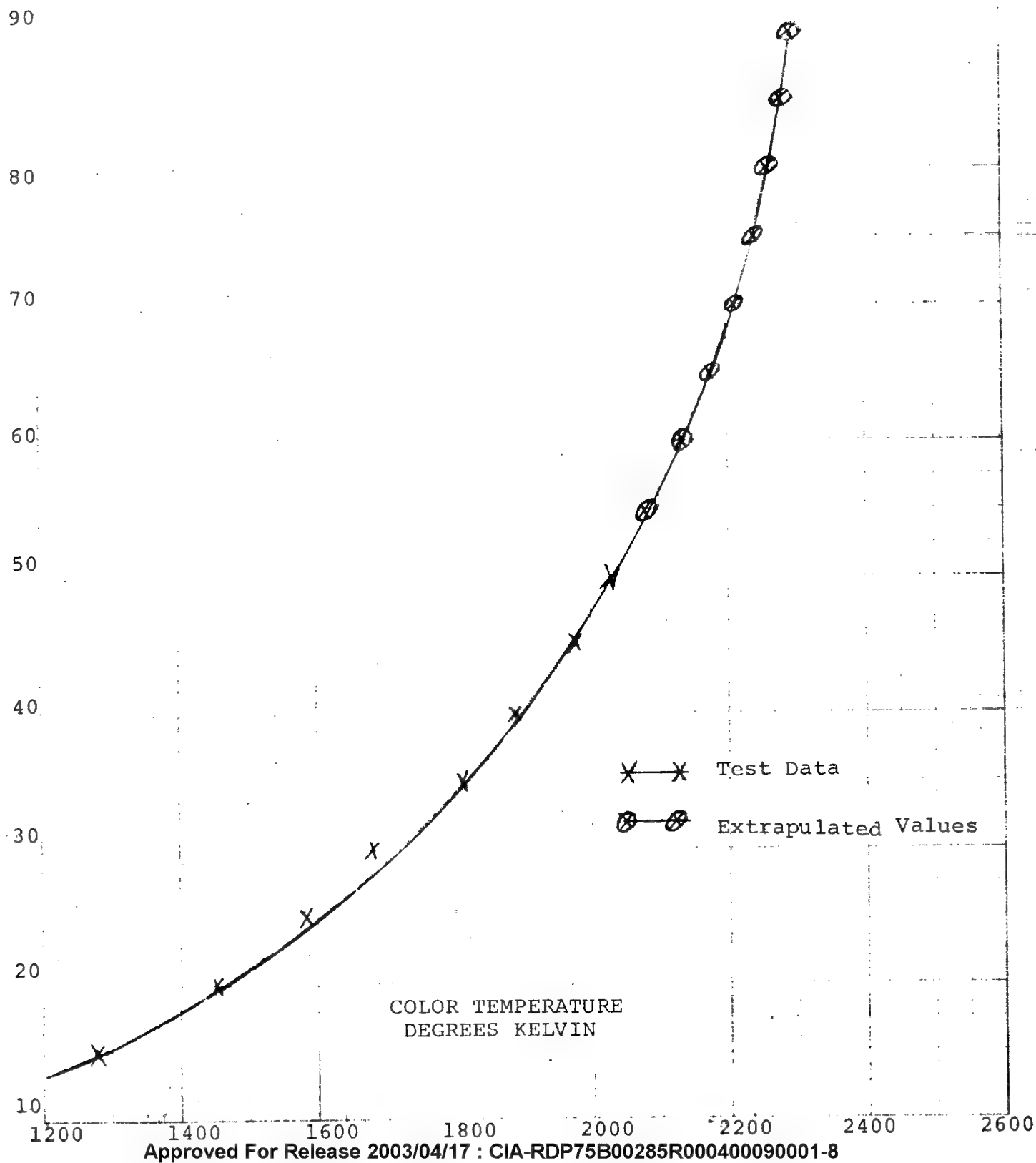
TABLE V

PROPERTIES OF TUNGSTEN

COLOR TEMP. $^\circ$K	ACTUAL TEMP $^\circ$K	TOTAL EMISSIVITY	PEAK ENERGY W_λ	PEAK WAVELENGTH λ	TOTAL EMITTED ENERGY W
2030	2000	0.260	10.92	1.448	23.66
2135	2100	0.270	14.31	1.37	29.97
2240	2200	0.279	18.69	1.316	37.39
2345	2300	0.288	24.18	1.259	45.94
2450	2400	0.296	30.49	1.207	55.65
2555	2500	0.303	38.18	1.159	67.27

$W = \varepsilon \sigma T^4$ watts/cm^2 source, Stefan-Boltzmann Law

$\lambda = \dfrac{K}{T}$ wavelengths in microns, Wein's Displacement Law showing peak radiation wavelengths

$W_\lambda = \dfrac{\varepsilon\, c_1}{\lambda^5 \left(e^{c_2/\lambda T} - 1 \right)}$ watts/cm^2 source – Planck's Law showing energy emitted at peak radiation wavelength

In the above equation:

$K = 2897\mu$ deg.
$c_1 = 3.7402 \times 10^{-2}$ watts cm^2
$c_2^1 = 1.4385$ cm. deg.

Chem. Lab B

GRAPH #3

Watts/2 X 10^{-2}
Microns

SPECTRAL DISTRIBUTION OF TUNGSTEN
FILAMENT QUARTZ LAMP FOR VARIOUS
COLOR TEMPERATURES

MICRONS
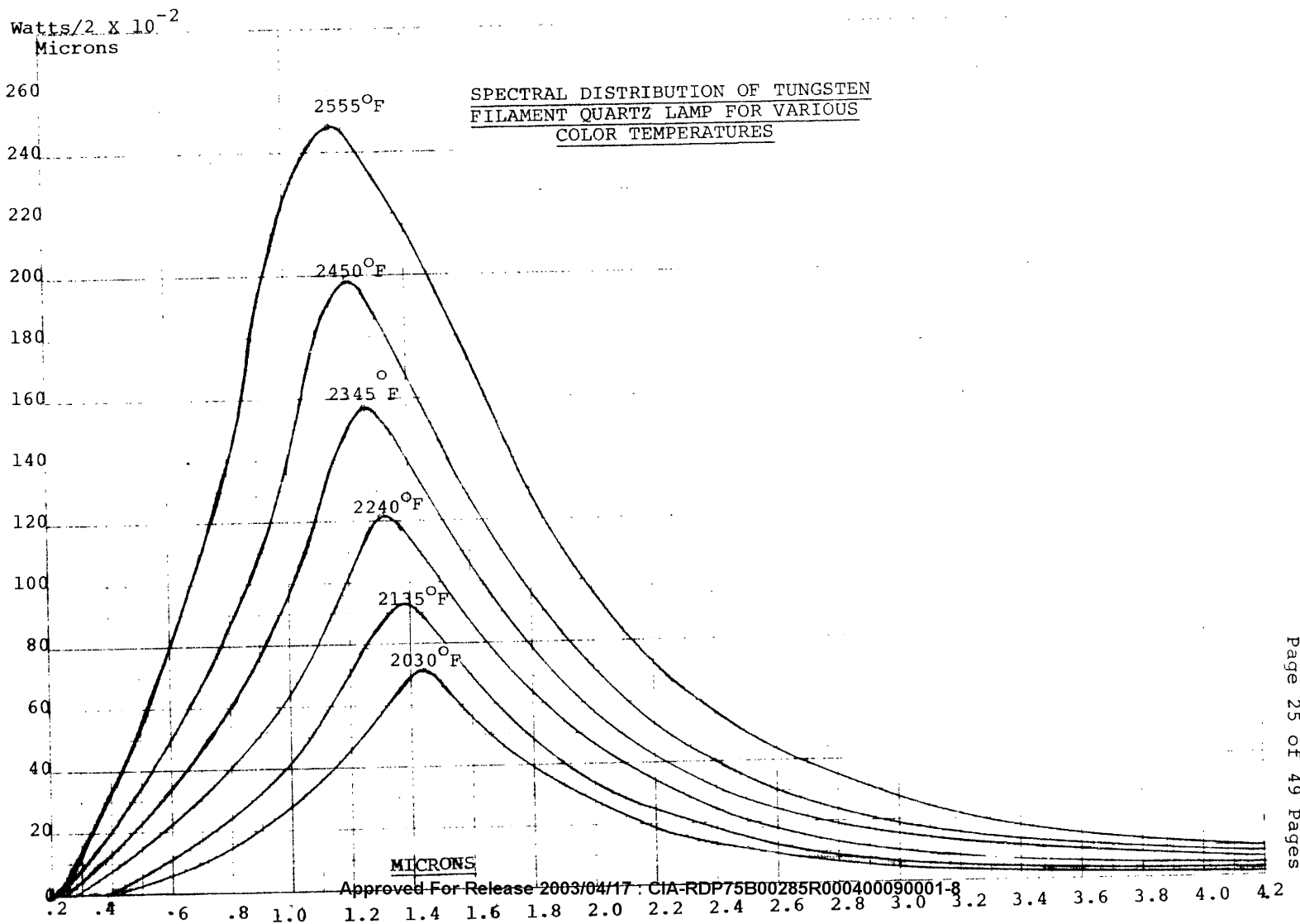
TABLE VI

SPECTRAL DISTRIBUTION OF ULTRA-VIOLET
LAMP

WAVE LENGTH BAND μ		PRINCIPLE LINES	WATTS OF RADIANT ENERGY
	.22 - .23	–	.45
	.23 - .24	–	.55
FAR	.24 - .25	–	1.20
UV	.25 - .26	.2537	3.00
	.26 - .27	.2652	1.99
	.27 - .28	–	.37
		TOTAL	7.65
	.28 - .29	.2804	1.82
MIDDLE	.29 - .30	.2967	1.28
UV	.30 - .31	.3022	2.28
	.31 - .32	.3131	4.43
		TOTAL	9.81
	.32 - .33	–	.28
	.33 - .34	–	.61
	.34 - .35	–	.16
NEAR	.35 - .36	–	.21
UV	.36 - .37	.3654	7.05
	.37 - .38	–	.20
	.38 - .39	–	.28
		TOTAL	8.79
	.40 - .41	.4047	1.74
	.41 - .43	–	.26
	.43 - .44	.4358	4.18
	.44 - .54	–	0.64
	.54 - .55	.5461	4.65
	.55 - .57	–	0.29
	.57 - .58	.5780	5.05
	.58 - .76	–	1.09
			17.90

Chem. Lab B

SPECTRAL DISTRIBUTION
OF
ULTRAVIOLET LAMP

TABLE OF RESULTS   TABLE VII

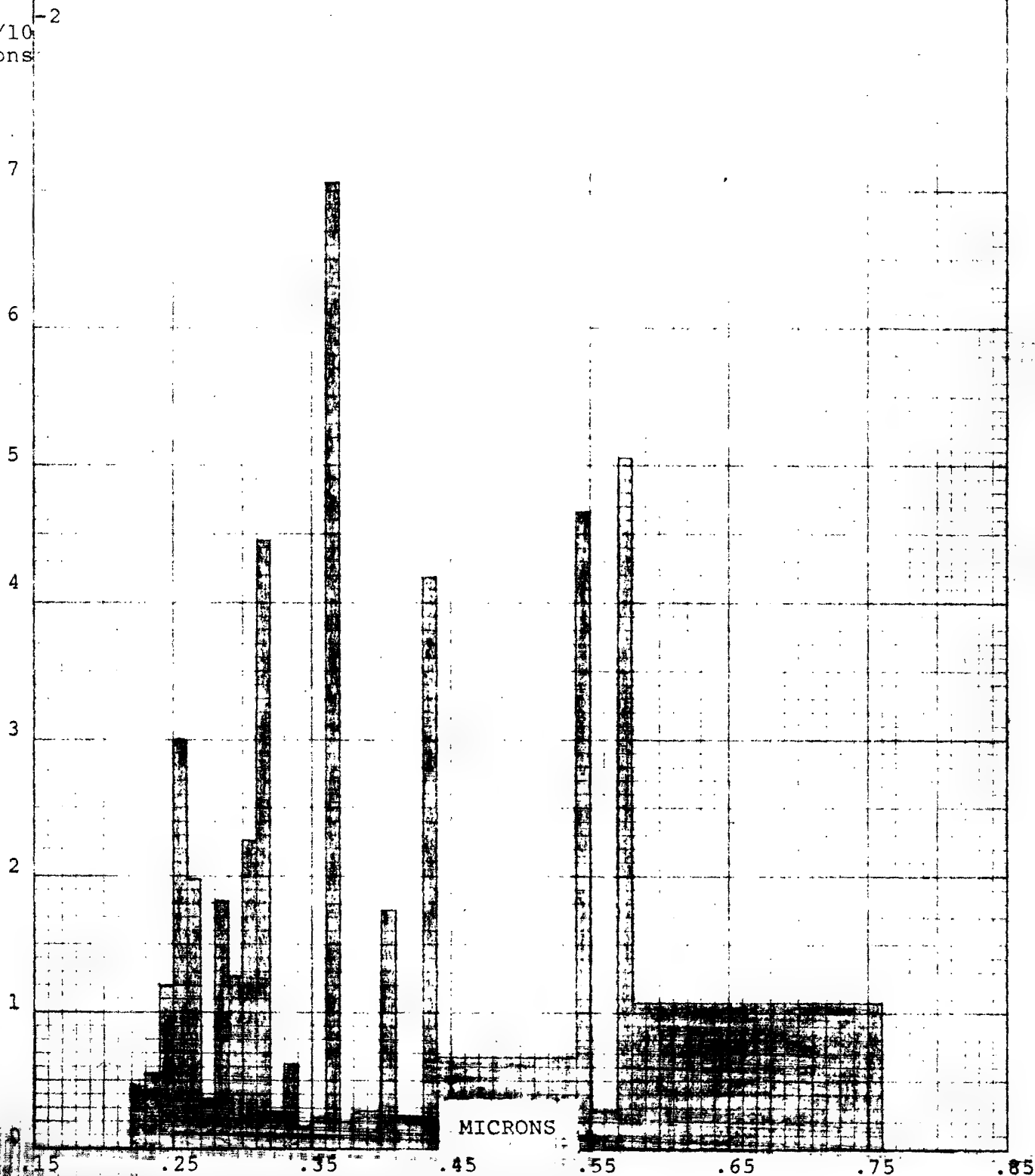| TEST CONDITIONS	1a	1b	1c	1d	2a	2b	2c	2d	3a	3b	3c	3d	4a	4b	4c	4d	5a	5b	5c	5d
Test flow rate, scfm	2.7	3.88	2.7	3.88	2.7	3.88	2.7	3.88	2.7	3.88	2.7	3.88	2.7	3.88	2.7	3.88	2.7	3.88	2.7	3.88
Corresponding suit flow rate, scfm	12.5	18	12.5	18	12.5	18	12.5	18	12.5	18	12.5	18	12.5	18	12.5	18	12.5	18	12.5	18
Back pressure, in. Hg	5.3	20.3	5.3	20.3	5.3	20.3	5.3	20.3	5.3	20.3	5.3	20.3	5.3	20.3	5.3	20.3	5.3	20.3	5.3	20.3
Ventilation entrance temp. ^{o}F	65	64	65	68	70	68	61	68	55	72	65	73	65	72	70	75	72	72	74	70
Exhaust temp. ^{o}F	89	80	88	76	91	77	83	75	80	78	89	84	90	84	86	85	100	81	99	86
Ozone concentration, pphm	6	6	6	6	6	6	6	6	6	6	6	6	6	6	6	6	6	6	6	6
Skin-underwear gap, in.	1/8	1/8	0	0	1/8	1/8	0	0	1/8	1/8	0	0	1/8	1/8	0	0	1/8	1/8	0	0
Approx. compression gm/cm^2	N/A	N/A	30	30	N/A	N/A	30	30	N/A	N/A	30	30	N/A	N/A	30	30	N/A	N/A	30	30
Final temp. of underwear liner, ^{o}F	200	149	140	125	180	75	138	123	123	85	145	129	162	142	152	130	122	101	190	161
Initial voltage	82	85	84.5	90	83	88	82	84	90	88	86	84.5	82	83	80	79	83.5	89.5	80	89
Final average voltage	81	86	79	83	85	93	82	83	85	82.5	82	84	79	78	78	79	84	79.5	81	81
Surface reflectivity % @ 1 micron	57.3	57.3	57.3	57.3	67.7	67.7	67.7	67.7	59.4	59.4	59.4	59.4	52.6	52.6	52.6	52.6	52.6	52.6	52.6	52.6
Final heat flux, $watt/cm^2$	.0293	.0301	.0288	.0298	.0301	.0309	.0293	.0298	.0301	.0293	.0293	.0298	.0288	.0277	.0277	.0288	.0298	.0288	.0293	.0293
Total test time, min.	34	34	26	32	34	40	36	34	34	34	34	34	34	30	34	34	34	34	34	34
Time required to reach $200^{o}F$	9	16	9	7	22	32	18	8	9	5	6	7	4	3	3	3	3	3	3	3
Time for which surface temp. exceeded $200^{o}F$	25	18	17	25	12	8	18	24	25	29	28	27	30	27	31	31	31	31	31	31
Final surface temp. ^{o}F	247	227	233	238	217	212	233	236	242	230	252	240	255	255+	255+	255+	255+	255+	255+	255+
Final skin temp. ^{o}F	95	78	96	81	100	74	100	90	94	78	104	90	111	93	117	95	115	96	127	90
Final temp. gradient	152	149	137	157	117	138	133	146	158	152	148	150	144	162	138	160	140	159	128	155

GRAPH #5   Page 29 of 49 Pages

TIME VS. TEMPERATURE GRAPH

Skin temperature vs. time for uncompressed condition at low flow ventilation.

Temperature in °F

Test #1a
Test #2a
Test #3a
Test #4a
Test #5a

EXPOSURE TIME (MINUTES)

TIME VS. TEMPERATURE GRAPH

Skin temperature vs. time for
uncompressed condition at high
flow ventilation.

Temperature in °F

EXPOSURE TIME (MINUTES)
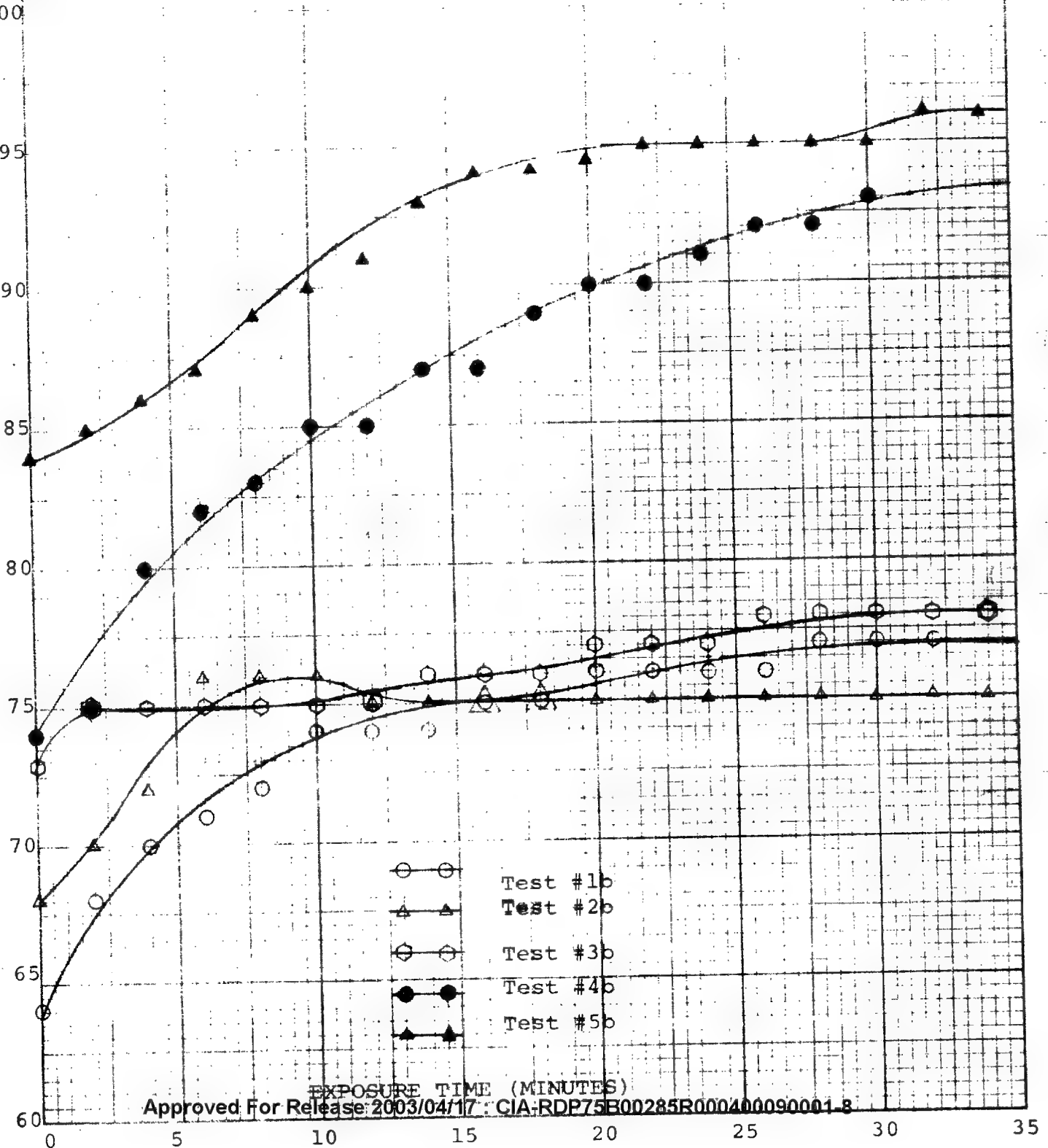
GRAPH #7

TIME VS. TEMPERATURE GRAPH

Skin temperature vs. time for
compressed condition at low
flow ventilation.

Temperature
in °F

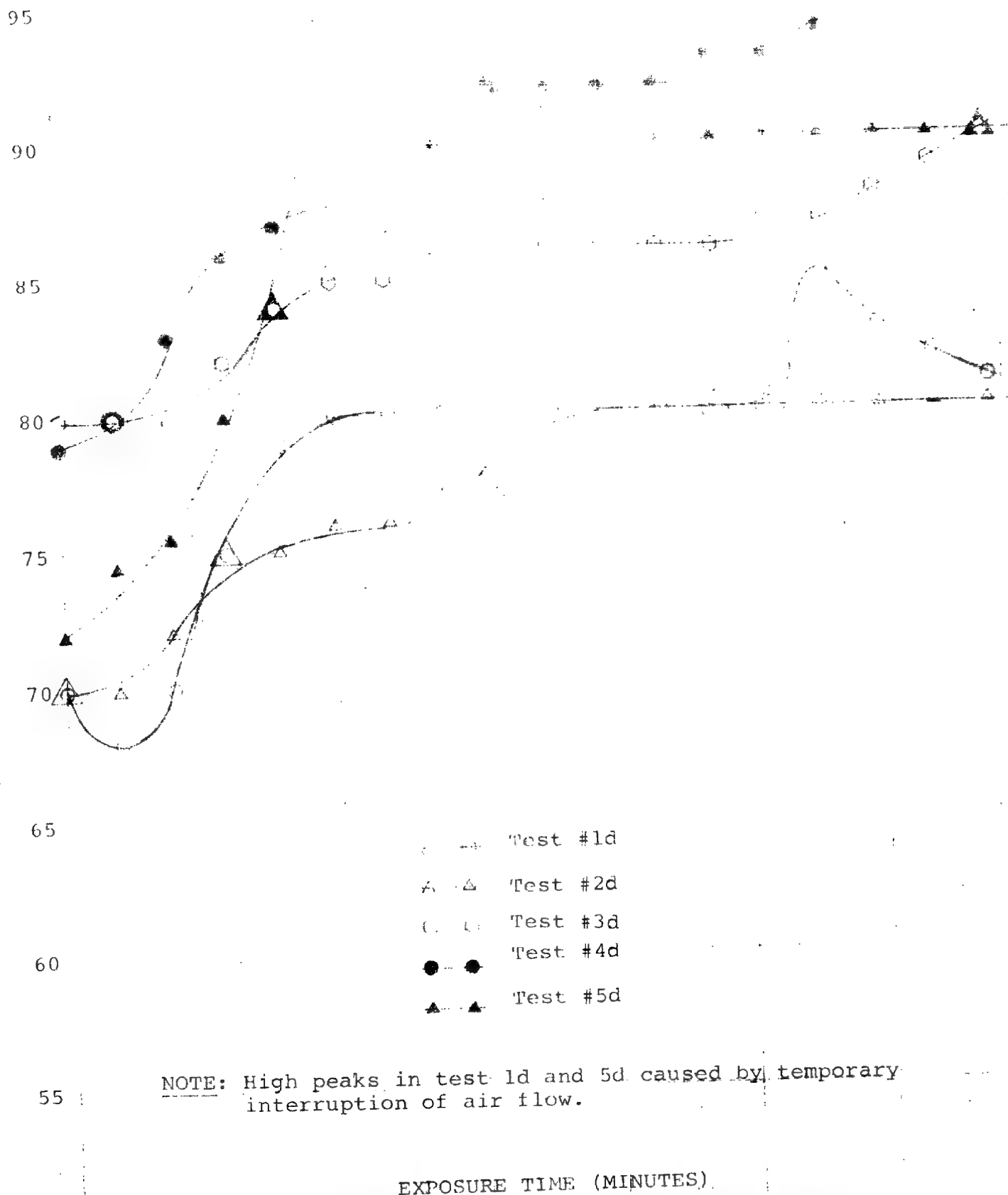|		
⊖——⊖	Test #1c
△——△	Test #2c
⦶——⦶	Test #3c
●——●	Test #4c
▲——▲	Test #5c

EXPOSURE TIME (MINUTES)

GRAPH #8   Page 32 of 49 Pages

Temperature
in °F

TIME VS. TEMPERATURE GRAPH

Skin temperature vs. time for
compressed condition at high
flow ventilation.

95

90

85

80

75

70

65

60

55

50

	Test #1d	
	Test #2d	
	Test #3d	
	Test #4d	
	Test #5d	

NOTE: High peaks in test 1d and 5d caused by temporary
interruption of air flow.

EXPOSURE TIME (MINUTES)

0   5   10   15   20   25   30   35
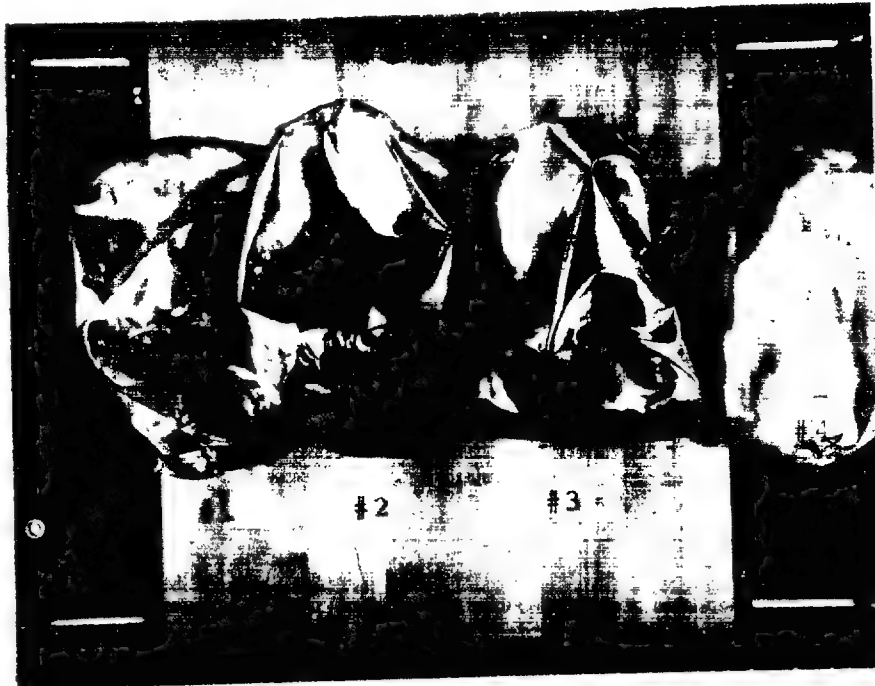
FIGURE #9

COVERALL TEST SPECIMENS AFTER THE TEST

#1 - Standard 3M process Scotch Shield
#2 - 3M laminated process (stiff)
#3 - DC Heat Shield Type 2, ACS-1440C
#4 - 6 ounce HT - not aluminized

NOTE: The picture relates to description only
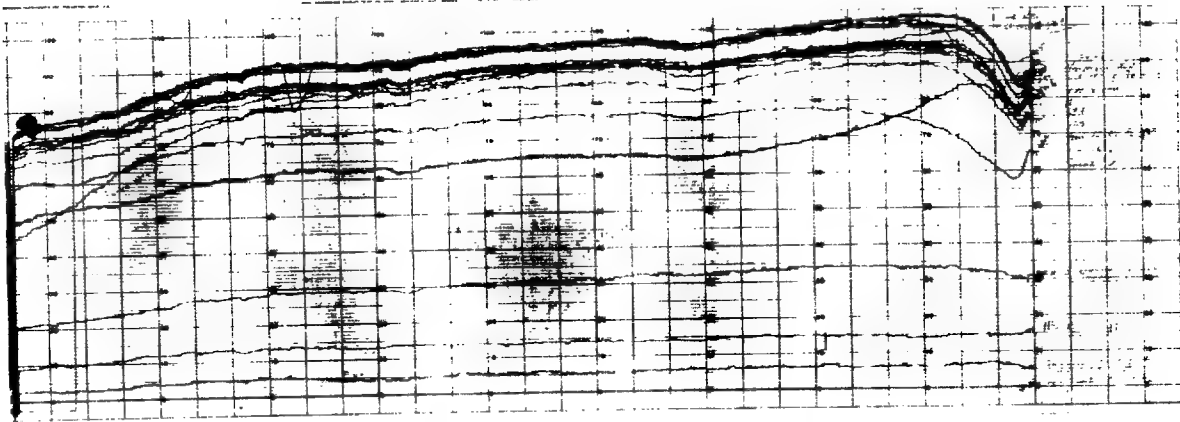and not to numbers of specimens.

Chem. Lab B

CHART #1

VAR 100% Reflectance of Reference Mirror Between
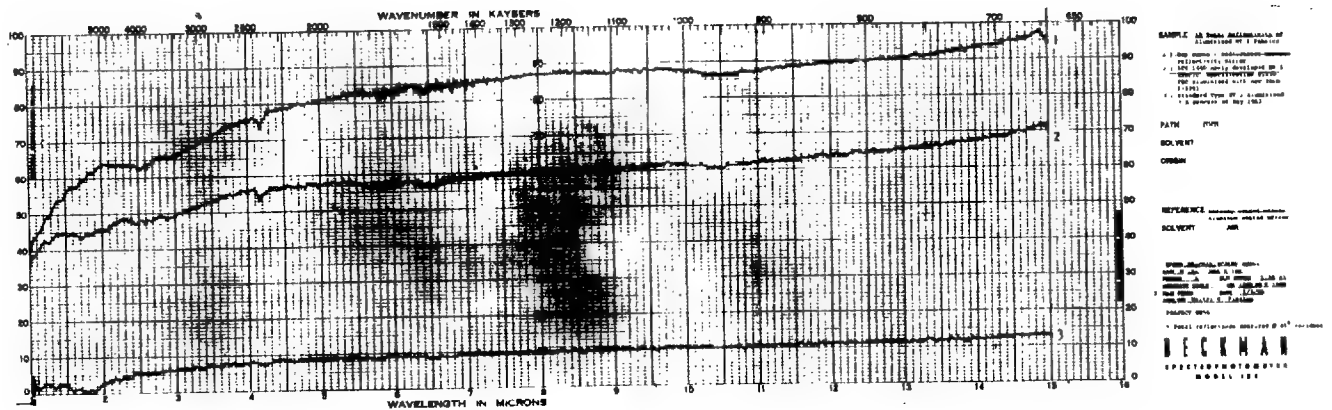15° and 80° of Incident

CHART #2

Total Reflectivity of Standard Aluminized HT-1 (3)
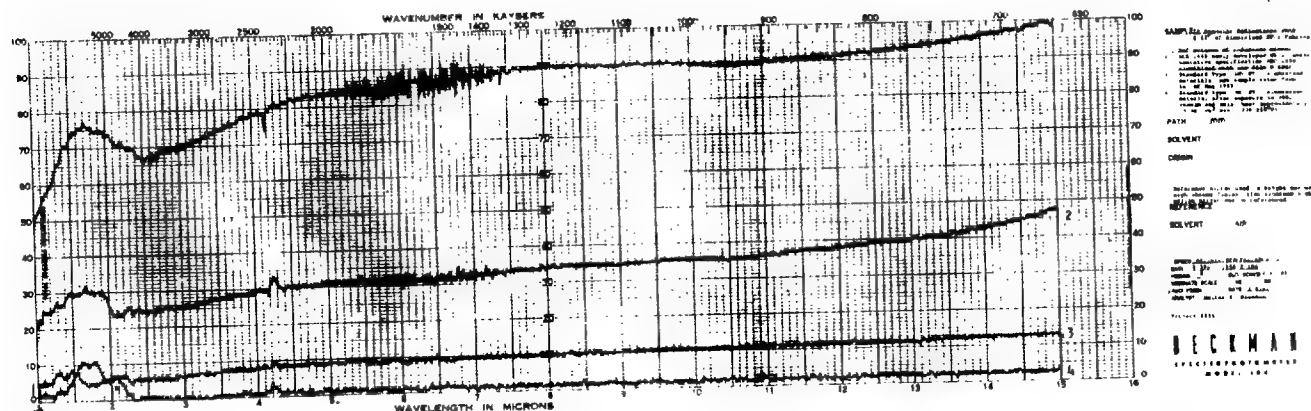and Newly Developed Heat Shield Type 2

Chem. Lab B

CHART #3

Total specular reflectance (VAR) showing at bottom:
1. Line 1 - 100% reference line
2. Line 2 - new DC aluminized HT process ACS-1440C
3. Line 3 - HT aluminized 3M process before high
            altitude thermal study phase I
4. Line 4 - same as line 3 except after thermal
            study phase I

CHART #4

Attenuated total reflectance (ATR)
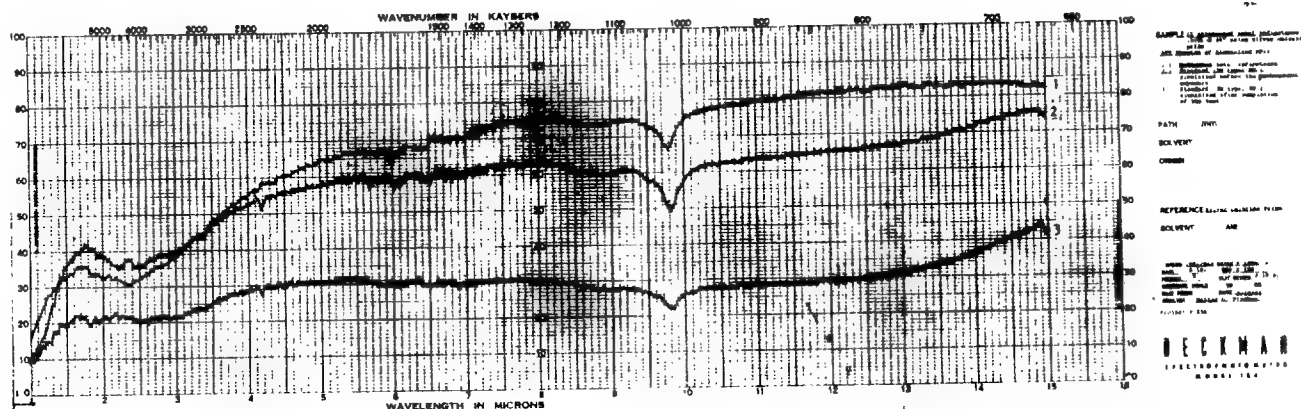1. Line 1 - 100% reference line
2. Line 2 - standard 3M process before thermal
            environmental exposure
3. Line 3 - same as line 2 except after environ-
            mental exposure
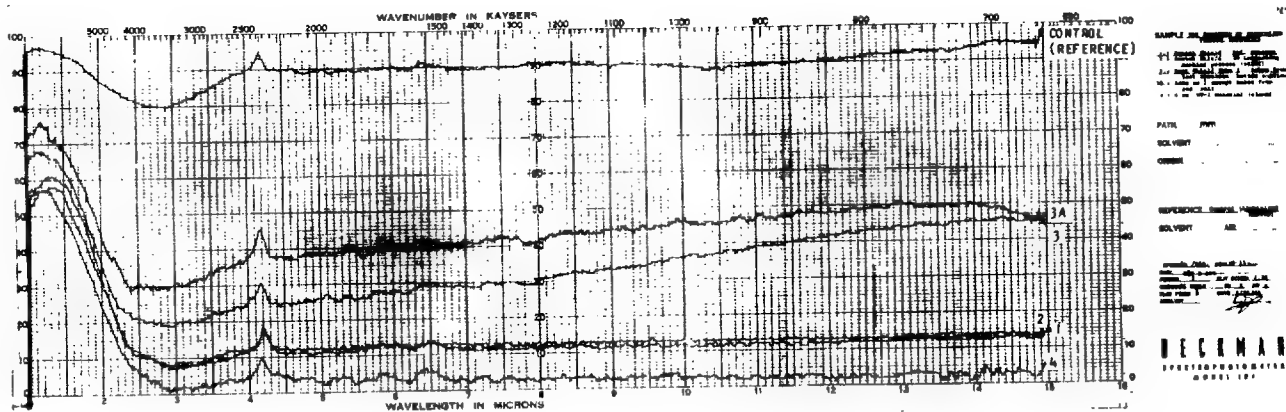
Chem. Lab B

CHART #5

VAR Reflection Spectrum of all Test Materials
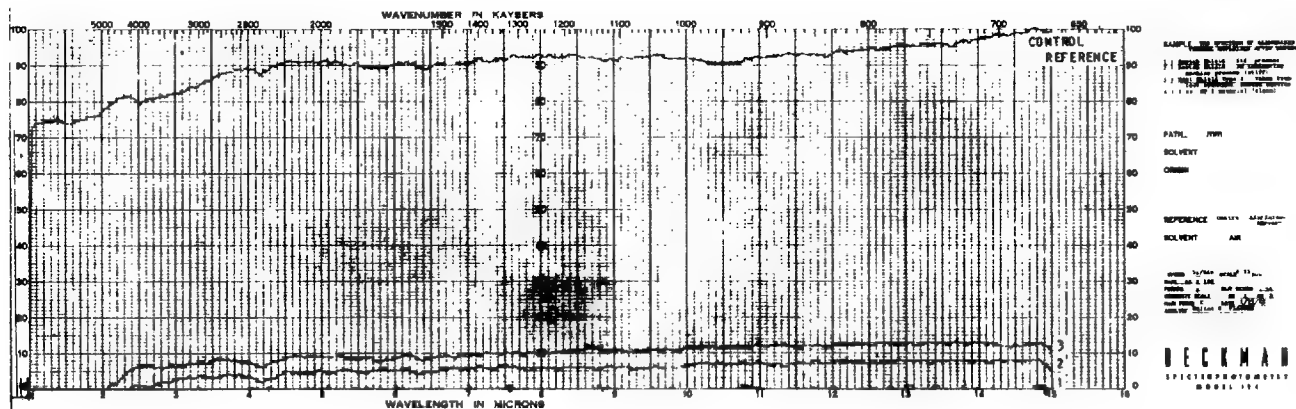Before Environmental Tests

CHART #6

VAR Reflection Spectrum of all Test Materials
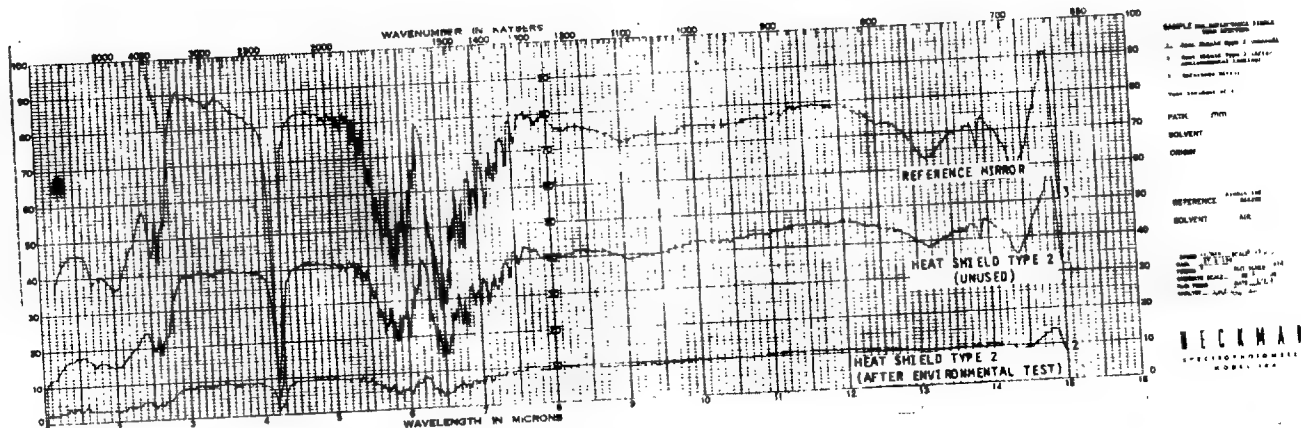After Environmental Tests

Chem. Lab B

CHART #7

VAR High Resolution Reflectivity (Single Beam)
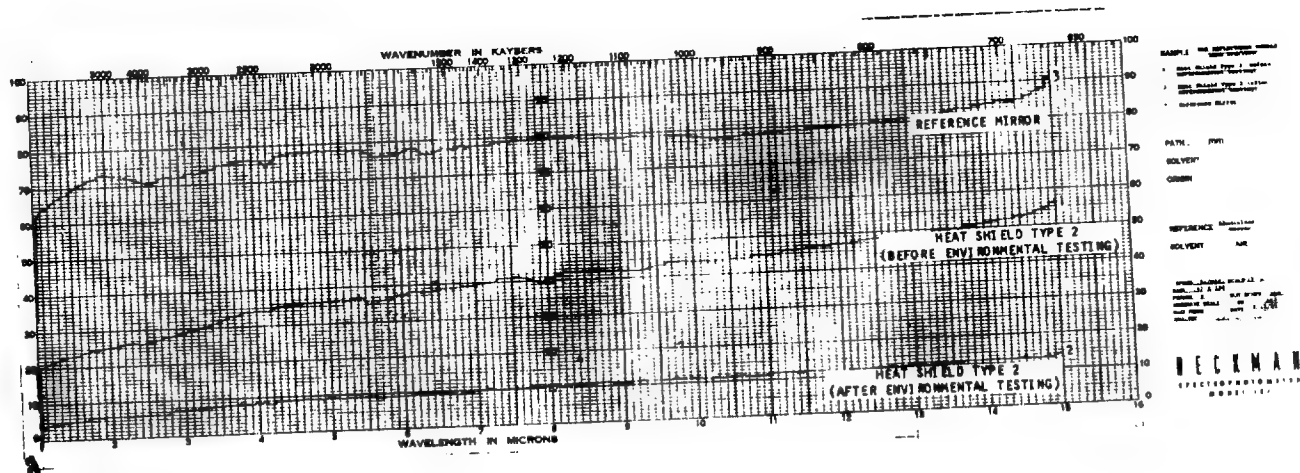of Heat Shield Type 2 ACS-1440C

CHART #8

VAR High Resolution Reflectivity (Double Beam)
of Heat Shield Type 2 ACS-1440C

Chem. Lab B

TABLE VIII

TOTAL ENERGY REFLECTANCE FOR ORIGINAL HEAT SHIELD TYPE 3

λ BAND IN μ	% OF TOTAL INCIDENT ENERGY CONTAINED IN BAND	AVERAGE % REFLECTANCE OF BAND				% OF TOTAL INCIDENT ENERGY REFLECTED			
		DC ORIGINAL	DC EXPOSED	3M ORIGINAL	3M EXPOSED	DC ORIGINAL	DC EXPOSED	3M ORIGINAL	3M EXPOSED
1.0-1.5	20.67	73	0	58	0	15.09	0	11.99	0
1.5-2.0	20.89	60	0	47.5	0	12.53	0	9.92	0
2.0-2.5	15.18	44	5	25	.05	6.68	.75	3.80	.01
2.5-3.0	10.50	37	8	11.5	.05	3.88	.84	1.21	.01
3.0-3.5	6.92	38.5	8.5	10	.05	2.66	.58	.69	< .01
3.5-4.0	4.91	40	9.0	11.5	.05	1.96	.44	.56	< .01
4.0-4.5	3.37	42	9.0	12.5	.05	1.42	.30	.42	< .01
4.5-5.0	2.42	42	9.5	13	.05	1.02	.23	.31	< .01
5.0-5.5	1.76	44	9.5	12.5	.05	0.77	.17	.22	< .01
5.5-6.0	1.32	44.5	9.5	13.5	.05	0.59	.13	.18	< .01
6.0-6.5	1.00	44.5	9.5	14.5	.05	0.45	.10	.15	< .01
6.5-7.0	0.78	45.5	10.5	14.5	.05	0.35	.08	.11	< .01
7.0-7.5	0.61	47	11	13	.05	0.29	.07	.08	< .01
7.5-8.0	0.48	46.5	11	12.5	.05	0.22	.05	.06	< .01
8.0-8.5	0.39	46.5	12	13	.05	0.14	.05	.05	< .01
8.5-9.0	0.31	48.5	12	13	.05	0.15	.04	.04	< .01
9.0-9.5	0.26	49	12	13	.05	0.13	.03	.03	< .01
9.5-10.0	0.22	50.5	12.5	12.5	.05	0.11	.03	.03	<< .01
TOTAL	91.99					48.44	3.89	29.85	0.1 (approx.)

Calculated reflectance from spectrum charts and data
presented in this table was accomplished as follows:

$(\lambda_1 - \lambda_2)$ as analyzed spectrum

WHERE:

$$\frac{R_0 - R_\lambda}{R_0} \times 100 = \%$$

$$W = \frac{\int_0^{\lambda_2} W_{\lambda 2} \, d\lambda}{\int_0^\infty W \, d\lambda} - \frac{\int_0^{\lambda_1} W_{\lambda_1} \, d\lambda}{\int_0^\infty W \, d\lambda}$$

4.0   Discussion of Errors and Errors Involved in Test:

In the test and simulation described herein, certain assumptions, inaccuracies, extrapolations and errors were inherent in the system. These variations from true data will cause discrepancies in the final reported results. These discrepancies with their cause, probable effects and method of remedy are listed below:

4.1   Chamber Pressure:

The vacuum chamber used to simulate the desired altitude pressure was the chamber of a very high vacuum system. For this test, the diffusion pump was closed off from the system and only the mechanical pump was used. The chamber pressure was measured with a thermocouple gage. To all practical extent, the chamber pressure was not controlled accurately during the test. Normally, control would be achieved through the use of very fine needle valves. However, in the tests performed there were too many variables present. Variables existed such as trapped water vapor, off-gassing; different sample leak rates for each material, flow rate and temperature tested. Precise control of chamber pressure under these conditions would have added many hours or perhaps days to each test performed in the program which was already surpassing its time deadline. Therefore, the practical low pressure of the system was the pressure that was used even though it varied from test to test.

This pressure change caused a variation in the simulated altitude. The pressure varied from 500 to 5,000 microns. These pressures represent altitudes from approximately 110,000 to 165,000 feet while the test requirements were 25,000 to 100,000 feet. (see Graph 1 and Table III)

Chem. Lab B

4.2 Ventilation:

Ventilation was controlled in the test by a needle valve and measured by a flow meter. The flow meter used was calibrated from 2.5 to 17 scfm @ 70 psig air. Therefore, the low ventilation rates of 1.73 scfm corresponding to a suit flow rate of 8 scfm could not be run. (see Tables I and II)

Due to high back pressure developed at the higher flow rates greater than 3.88 scfm (18 scfm suit flow equivalent) were not used. At this flow rate the back pressure was 20.3 in. Hg (9.97 psi). The large back pressure was caused by a small diameter oriface and piping used. These diameters were limited by the size of the chamber and samples.

Other variables in ventilation which could cause apparent discrepancies in result data include; different temperatures of entrance gas and temporary interruption in ventilation gas. The temperature of the ventilation gas was dependent upon the immediate history of the gas storage tank. This is, if the tank was just delivered or the test made early in the morning, the gas could be quite cool, but if the test was made in the afternoon, the gas would be warmer. Temperature variation should be eliminated by the use of a constant temperature gas warmer. Temperature differences of up to $20^{\circ}F$ were noted. A constant temperature gas warmer was not used in this test because it was felt that the advantages did not outweigh the loss in time that would occur from acquiring and installation of such a unit into the system. (see Table VII)

The interruption of gas flow was caused by the changing of empty compressed air tanks. This could be eliminated by using supply tanks connected with a "Y" connection to the system. (This type of set up would also be required for higher flow rate testers.)

Chem. Lab B

4.3 Supply Voltage and Color Temperature:

The supply voltage to the IR lamp had a tendency
to vary. This variation could cause an incorrect
average voltage reading. It was from this aver-
age voltage reading that the color temperature
and, therefore, the heat flux was calculated.
An error of 3 volts in the average voltage would
cause an error of approximately $10^\circ K$ in color
temperature.

Heat flux is dependent upon the forth power of
the color temperature. Therefore, a considerable
change in heat flux would be realized by a small
error in voltage reading. The variation of the
voltage itself could not be overcome, as it was
caused by the equipment used in the electrical
circuit. The only method of overcoming this
problem would be the use of a recording volt-
meter. With this type of instrument, many more
voltage readings could be used to obtain the av-
erage voltage. This would eliminate the use of
several instantaneous readings.

To determine the temperature, data for the volt-
age vs. color temperature graph, an optical pyro-
meter was used. This pyrometer had an upper
range limit of approximately $3200^\circ F$ ($1983^\circ K$).
This limit was reached at approximately 50 volts.
Because the lamp was run at higher voltage,
further values had to be extrapulated from the
lower values. These extrapulated values could
lead to fairly high errors in heat flux. This
area should be further studied through the use
of a higher range pyrometer.

Chem. Lab B

4.4 Reflectivity of Surface:

As shown by the results of this test, the re-
flectivity of the surface is very important in
relation to the amount of heat traveling into
the test specimen. In the test performed for
this report, one sample of each material was
used for all tests performed on that material.

After each test was completed, the surface had
degraded to some extent, some material more than
others. This degradation in the surface re-
flectivity caused a larger amount of heat ab-
sorption in the later tests on a material than
on the prior tests. This resulted in higher
exterior and interior temperatures than would
otherwise be experienced. The estimated in-
ternal temperature effect would be 2-5°F.
These changes in reflectivity can be noted on
the Charts on pages 34-37.

The reflectivity of the various materials was
measured on a Beckman IR4 Spectrophotometer.
This instrument recorded the reflectivity from
2 to approximately 15 microns. However, the
most important wavelength emitted by the lamp
was the wavelength band at which the peak energy
was emitted.. This band was between 1.1 and 1.5
microns. Therefore, it is obvious that the
reflectivity in the UV and visible NIR spectrums
remain unknown to us.

Chem. Lab B

5.0 CONCLUSION:

Within the framework of the analysis presented in
this report, it is obvious that most of the discom-
fort experienced by the pilots traveling at high
velocity was due to the radiational heat. Although
the cockpit area is constantly pressurized and vented
to provide the required comfort within the cockpit,
the pilots wearing the P.P.A. continue to experience
unbearable heat leak through the thermal garment.

It is evident from the test data that the heat leak
was concentrated in the areas under compression and
tension or direct contact of materials with the skin.
The areas most vulnerable to immediate heat penetra-
tion would be the shoulders, elbows, hands, knees and
possibly the chest if compressed by a parachute har-
ness or other hardware.

This phenomenon of heat leak into the P.P.A. is be-
lieved to be primarily due to direct impingment of
the solar flux from the P.P.A. and indirect reflection
from the instrument panels or other grey bodies.

As shown in the summary data on page 28, as much as
$15^\circ F$ can be emitted if the surface of the aluminized
garment is new, dust free, and of high reflectivity
surface.

Material in service prior to the introduction of the
new ACS-1440C aluminized "NOMEX" reflects the reasons
for experienced heat leak.

Chem. Lab B

This material has demonstrated low reflectivity
value (see Chart   ) even when it was unused.
After subjecting this material in the form of a
composite in high altitude chamber, it was
apparent that the temperature rise of the skin
is extremely rapid using standard ventilation (8
scfm).

High ventilation, however, (see Graph 8) has helped
to reduce the skin temperature slightly providing
that the material was not in direct contact with the
skin. Compressed material has shown very slight or
no change at all in temperature by increasing the
ventilation. Analysis indicates that this is real-
istic because although ventilation has been increased,
very slightly, more airflow was observed in the com-
pressed areas.

In evaluating various reflectivity surfaces of al-
uminized thermal garments, it was evident that cur-
rently developed GT-1 aluminized fabric was substan-
tial improvement in emissivity and reflectivity,
(see Table VIII)

The accurate values of reflectivity and emissivity
could not be determined of the new heat shield type
because of Spectrophotometer limitations. The pre-
sent spectrophotometer accurate range is from 2 to
14 microns and in order to establish accurate data
and calculating total reflective or emissive effici-
ency, additional range between 200 and 2500 milli-
microns is required.

The results of I. R.   Simulation test, however,
have substantiated (see Table VII) that the new Heat
Shield Type ACS-1-400 is improved thermal barrier
due to higher surface reflectivity of the thermal
garment (see Graph 5). This can be seen by review-
ing the data on Graph 5 which indicates that not only
the T was higher but during the test it was nec-
essary to increase the power to the solar lamp in
order to maintain the surface temperature between
200 and 250°F.

Chem. Lab B

The altitude during which this test was conducted has
not been precise, within the range of the test pro-
file, namely; 75, 80 to 180,000 feet because of leaks
developed in the pressure area and other reasons ex-
plained in "Discussion of Testing Problems and Errors".

However, the pressure was maintained between 500 and
5,000 microns which is equivalent to the altitude of
110,000 to 165,000 feet. This we believe has not
changed or effected the data that could be considered
unrealistic. It is true that the high altitude utiliz-
ed has effected the back pressure and consequently the
heat transfer, however, a similar situation would be
experienced when the P.P.A. is worn by the pilot in a
sitting position. Throughout the testing, the surface
temperature of the thermal garment was maintained at
200 to $250°F$. This was accomplished with a $.03$ cal/
cm^2/sec. equivalent to the solar flux spectrum distri-
bution which is between $.2$ and 15 microns. (see Graph 3).

In evaluation of simulated P.P.A. and the environ-
ment, the solar flux selected was based on information
available indicating that the test programs and actual
flights were experiencing the 200 to $250°F$ garment
surface temperature. (See Table VII)

First of all in comparing the aluminized surface effect
on skin temperature, it could be said that the Heat
Shield Type 2, ACS-1440C was the best. (see Graph 7)

The added insulation of Dacron-wool increases the
thermal balance even more effectively because of inter-
ference of heat conductivity through space. Mainly,
as the outside aluminized surface gradually oxidizes
and decreases in reflective efficiency, the added
insulation provided that extra shielding which pre-
vented the skin temperature to increase above the
critical level. This can be realized by comparing
the skin temperature of the standard material per the
same unit time vs. the test specimen.

Chem. Lab B

Two additional tests (see Graph 5) show that aluminiz-
ed material covered with plain white HT fabric in-
creases the emissivity of the material where 15^OF
skin temperature can be realized per equal unit of
time. The aluminized material being covered apparent-
ly serves as a conductor of heat rather than the re-
flector.

The elimination of aluminized material and using plain
HT fabric as outside garment with added dacron-wool
insulation doubles the heat leak per the same air
flow and unit time. (see Table VII)

Visual examination of materials after the environment-
al tests indicated various degrees of discoloration,
oxidation and stiffness. Severe oxidation and flake-
off was experienced on standard aluminized HT-1
sample 1. (see Fig. 9)

Also, considerable stiffness and oxidation was apparent
on sample 3 (3M). The plain HT-1 material used in the
test as the outside garment slightly stiffened and
very strongly yellowed. The complete degradation
effect can be noticed from the VAR spectrum reflect-
ance charts 5 and 6 using test reflection incident of
45°.

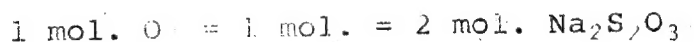Oxidation effect of aluminized surface can partly be
explained through the following reaction:

$$2AL + O_3 \xrightarrow{UV} AL_2O_3$$

and due to the air leak into the chamber a small
amount of ozone was generated as follows:

$$3O_2 \xrightarrow{UV} 2O_3$$

Chem. Lab B
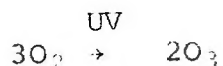
The ozone was detected only 6 pphm throughout the test using titrometer as shown on Figs. 6 and 7. This ozone detection was accomplished by the following reaction:

$$1 \text{ mol. } O = 1 \text{ mol. } = 2 \text{ mol. } Na_2S_2O_3$$

$$O_3 + 2KI + H_2O \rightarrow O_2 + I + 2KOH$$

$$I_2 + 2Na_2S_2O_3 \rightarrow Na_2S_4O_6 + 2NaI$$

In comparison to the altitude environment, it was concluded that 6 pphm of ozone used in the test represents only one-third of the expected effect in the actual flight or prolong storage.

In addition to ozone, the UV radiation and vacuum environment have effected the material by evaporation of lubricants or other components which contribute to stiffness and lack of adhesion.

Chem. Lab B

6.0 SUMMARY AND RECOMMENDATION:

In summarizing, it has been established that a significant degree of discomfort could be caused by the heat directly from the sun emitted through the windows.

Pressure points such as elbows, knees, etc., are most vulnerable and should be provided with additional protection such as anti-blocking material.

The reflective surface abraded, scuffed or contaminated will cause great deficiency in thermal balance, therefore, a clean and most durable aluminized material such as Heat Shield Type 2 is a prerequisite.

Flow rate or cooler air is of relatively little help if the above is not implemented. A plain coverall alone or a covering aluminized surface increases emissivity, higher heat conductivity and consequent discomfort, therefore, it is not recommended.

The heat reflection and transmission was not calculated or presented in BTU/ft.^{2}/hr./$^\circ$F because the total incident energy in the major wavelength regions (.2 to 2.5 microns) was not available. IR regions (2 to 15 microns) of spectrum was interpreted and the data is shown on Table VIII.

In view of the shortcomings experienced which were due to time allowed and not enough available equipment, it is proposed to implinent continuation of this program which would allow the development of a new anti-blocking material and complete thermal study of the P.P.A.

Chem. Lab B

REFERENCES

"Characteristics - Electrial and Radiant Energy", General Electric Company.

Gray, Dwight E, PhD., American Institute of Physics Handbook, Mc Graw-Hill Book Company, Inc., 1957.

Hackforth, Henry L., Infrared Radiation, Mc Graw-Hill Book Company, Inc., 1960.

Hodgman, Charles D., M.S., Handbook of Chemistry and Physics, Chemical Rubber Publishing Company, 1954.

"Product Heating with Infrared Lamps", General Electric Large Lamp Division.

"Study to Develop Design Criteria of the Solar Simulator Components for the Spacecraft Propulsion Research Facility", Fostoria Corp., Jan. 21, 1964.

"Tungsten Filament Lamps Various Color Temperature Spectral Distribution", General Electric Company, Lamp Division-Engineering Department.

Chem. Lab B